TURBULENCE CHARACTERISTICS AND ORGANIZED MOTION IN A SUBURBAN ROUGHNESS SUBLAYER

SUSUMU OIKAWA and YAN MENG
Environmental Engineering Department, Institute of Technology, SHIMIZU CORPORATION, No. 4–17, Etchujima, 3-chome, Koto-ku, Tokyo 135, Japan

(Received in final form 8 December, 1995)

Abstract. To investigate tubulence characteristics and organized motion within and above an urban canopy, field observations were conducted in July 1991 and November 1992 in Sapporo, Japan. The measurement heights were 5.4, 10.3, 18, 35 and 45 m above ground; the canopy height was 7 m. The profiles of σ_u peaked slightly above the canopy, while σ_v and σ_w had nearly uniform profiles. Vertical profiles of Reynolds stress $-\overline{u'w'}$ peaked slightly at 1.5 times the canopy height and decreased slowly with height thereafter. A four-quadrant analysis showed that sweep and ejection motions caused high-velocity fluid from above moves downward toward the surface and low-velocity fluid from below moves upward. An ensemble-averaging technique was used to isolate typical features of the flow and temperature fields. A time-height cross-section of velocity vectors and temperature contours showed details of the flow structures associated with temperature ramps. It has been noted that the organized motions play important roles in the transport of heat near the urban canopy, where the sweep motion causes negative temperature fluctuations and the ejection motion causes positive temperature fluctuations.

1. Introduction

Within an urban area, the many pollutant sources, including motor vehicles and chimneys, induce serious air pollution problems. The air pollution in urban areas is primarily emitted into two layers in the lowest part of the atmosphere. One layer, labeled the "urban canopy layer" by Oke (1976), is below the average height of buildings. The other layer was designated the "roughness sublayer" by Raupach *et al.* (1980), and the "transition layer" by Garratt (1978). The roughness sublayer is the layer in which roughness elements, such as buildings and trees, have a direct influence on the flow. The flow in this layer is complex because it is mechanically and thermally influenced by proximity to canopy elements. The diffusion process is strongly related to the turbulence structure in the atmosphere. Understanding the diffusion phenomenon requires a detailed understanding of the turbulence structure in both the urban canopy layer and the roughness sublayer.

There have been a limited number of observations of turbulence in and above the urban canopy layer; see, for example, Graham (1968); Bowne and Ball (1970); Brook (1972); Jackson (1978); Högström *et al.* (1982); Clarke *et al.* (1982); Uno *et al.* (1988); Rotach (1991); Oikawa (1993); Meng *et al.* (1993); Rotach (1993a,b); Roth and Oke (1993); and Roth (1993). The earliest measurements of turbulence in a city were made by Shiotani and Yamamoto (1950). They used five hot-wire anemometers on a 60 m tower in Tokyo, Japan, to measure turbulence and showed

Boundary-Layer Meteorology **74:** 289–312, 1995.

that the magnitude of turbulence intensity was very large and decreased with height. A similar result was obtained by Graham (1968) using vector vanes, which recorded the wind velocity along three coordinate axes in Fort Wayne, Indiana. He reported that the standard deviation of the azimuth angle at a low level at the city stations was about twice as great as that at rural stations. At the same site, Bowne and Ball (1970) observed that the ratios of the standard deviation of longitudinal, lateral, and vertical velocities to the friction velocity in an urban area were slightly larger than those at a rural site. Jackson (1978) measured turbulence with three-component propeller anemometers at heights ranging from 10 to 70 m at an urban site in Wellington, New Zealand. He found that the Reynolds stress showed a rapid decrease with height. These studies indicated that massive turbulence exists over urban areas, and that the turbulence level and the Reynolds stress decrease with height.

Duckworth and Sandberg (1954) measured the vertical temperature profile at urban and rural sites and showed that the temperature profile in the center of the city was nearly neutral at night, and that the noctumal inversion base was three times the average building height. They explained that the phenomena depended on thermal and mechanical effects near the surface of the urban site. A more detailed study of the nocturnal urban boundary layer was made by Uno *et al.* (1988) in Sapporo, Japan. They found that a layer of large turbulence and Reynolds stress extended up to three times the average building height, and that the inversion base over the urban center was approximately twice the average building height. They concluded that the formation mechanism of the nocturnal urban boundary layer was controlled by turbulent generation resulting from the effects of urban building elements rather than from heat emissions. That study suggested that wake production plays an important role in the formation of the nocturnal urban boundary layer.

However, a general description of the turbulence structure and organized motion over an urban site in near-neutral or unstable conditions has been lacking. Measurements near the urban canopy are difficult, and published observational data are very limited. Moreover, most of the published measurements of turbulence over urban canopies have been concerned with the behavior of mean turbulence statistics obtained by using standard statistical methods. Recently, Rotach (1993a), using four-quadrant analysis, found that momentum transport occurred through intermittent sweep and ejection events both within the street canyon and at its top. This implies the existence of organized motion over an urban area.

To clarify the vertical turbulent structure and organized motion within and above an urban canopy, a field study was conducted using three ultrasonic anemometer-thermometers at several heights in Sapporo, Japan. In this study, most measurements were taken within the roughness sublayer and, in addition, a small number of measurements were obtained above the roughness sublayer. This paper presents the results concerning (i) the turbulent statistics in and above the urban canopy, (ii) the process of generation of Reynolds stress near the canopy, and the ensemble-averaged image of the organized motions.

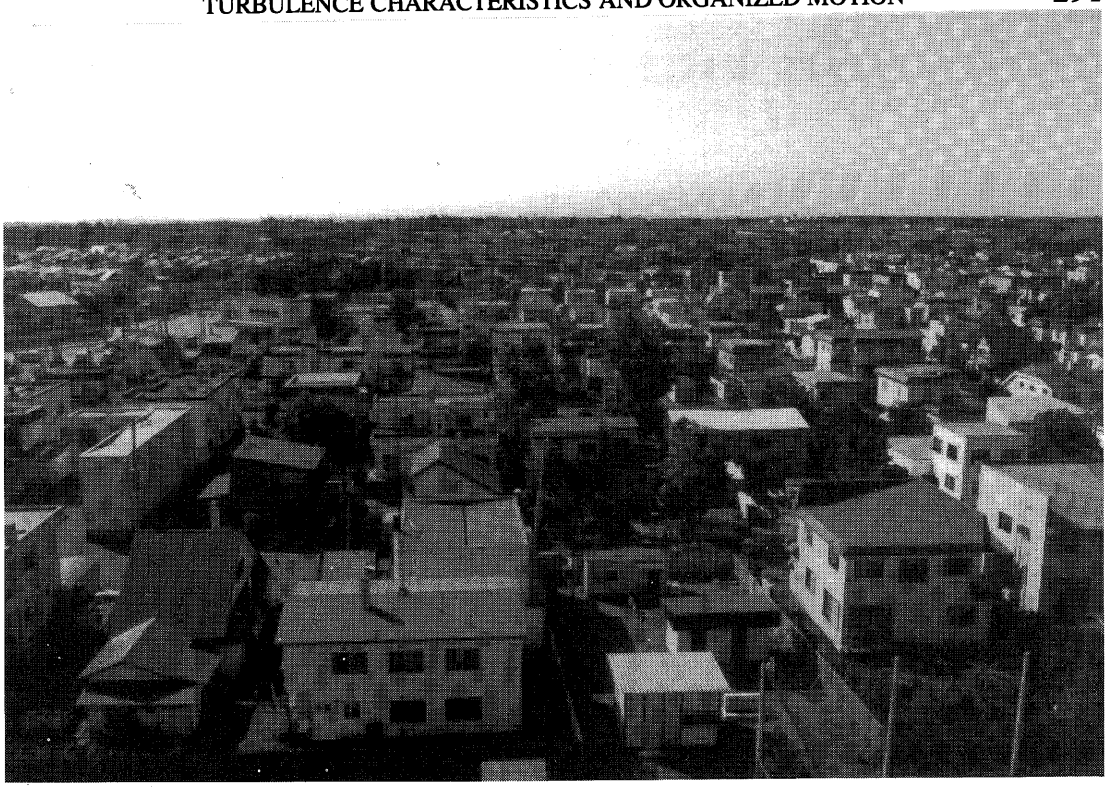

Fig. 1. Photographic view from the site facing northwest.

2. Observation Site and Experiments

2.1. Observation Site

The field study was conducted in Sapporo, Japan, in July 1991 and November 1992. The observation site was located at the northwestern end of a flat portion of the Ishikari Plain, where there was no distinct elevated terrain within a radius of about 3 km. Three km to the coast, the Plain fans out in a direction northwest to northeast. Mountains 1000 m in height wall the Plain from the western edge of the coast to the south. The site was located 10 km northwest of the center of the city. Residential dwellings, which are uniformly 7 m high, begin 30 m to the northwest of the site, and continue 2 km towards the coast. The percentage of area covered by houses (Ar) over total area (A) was 25%. Observations were conducted whenever the wind blew from the northwest. Southeast of the site are the soccer grounds of the Hokkaido Institute of Technology, which extend for 200 m and are bounded by a row of trees. Figure 1 is a photographic view from the site facing northwest.

2.2. Instrumentation

Turbulence characteristics were measured by 3-D ultrasonic anemometer-thermometers (Kaijo Denki Co., Ltd., velocity resolution: 0.005 m/s; temperature resolution: 0.025 °C). The ultrasonic anemometers were calibrated in a wind tunnel. All

data were collected on a digital recorder (TEAC Co., DR-F1) at a 10 Hz sampling rate. A 10-min averaging time was used for each run.

In this study, a specially designed ultrasonic anemometer-therrnometer, developed by Ogawa and Ohara (1982), was mounted on a mobile crane 45 m above the ground (sometimes 35 m). Although the ultrasonic anemometer is relatively new, its reliability has been demonstrated in several field studies (Ogawa *et al.*, 1986; Uno *et al.*, 1988; Ohara *et al.*, 1989). The anemometer sensor package was suspended 5 m from the top of the crane. This was done to prevent flow distortion by the crane support. The pitch of the anemometer sensor package was adjusted to zero before each run, and the inclination was measured during the observation period so that the data could later be corrected for yaw and pitch. The data were transmitted via an optical fiber cable system. A wind sock indicated the wind direction for the sensor package so that the latter could continuously face the approaching wind. This combination of the wind sock and the sensor package minimized possible distortion of the prevailing winds caused by any shadowing from the ultrasonic sensor supports. To verify the accuracy of this system, the sensor package was placed close to the sensor on an 18 m pole. The juxtaposition of these two sensors caused a systematic difference of 2 to 5% in mean wind speed and standard deviations of the three wind components.

The ultrasonic sensor (Kaijo TR-61A) positioned at $z = 18$ m has two orthogonal axes in the horizontal plane and one vertical axis. The partial shadowing of the acoustic path by the transducers affects the horizontal velocity field, resulting in underestimation of the wind velocity (Hanafusa *et al.*, 1982; Grant and Watkins, 1989). Field measurements by Grant and Watkins (1989) with the sensor (Kaijo TR-61A) showed that maximum errors in mean wind speed and standard deviations of the horizontal wind component were estimated to be between 10 and 20%. The maximum errors for wind directions occurred around $\Theta = 60°$ (the angle Θ between the wind vector and the center axis of the anemometer corresponds to flow along one of the measuring paths). However, the error was less than 5% for wind directions of $\Theta = 40°$, and negligible for $\Theta = 30°$. In the present study, wind directions were selected within $\Theta = \pm 40°$ of the central axis of the anemometer, and errors were less than approximately 5% for wind speed and standard deviations of the horizontal wind components. On the other hand, the Kaijo TR-61B ultrasonic sensors positioned at 5.4 and 10.3 m do not directly cause flow distortion in wind direction because the ultrasonic transducers do not exit in the horizontal plane. The errors for this sensor, which occurred as a result of flow disturbance caused by the three support frames, was less than 5% in all wind directions, as reported by Hanafusa *et al.* (1983).

2.3. Experimental Setup

Figure 2 shows a schematic of the field experimental setup. Ultrasonic probes at 18 and 10.3 m were mounted at the top of each pole, and a probe at 5.4 m was placed

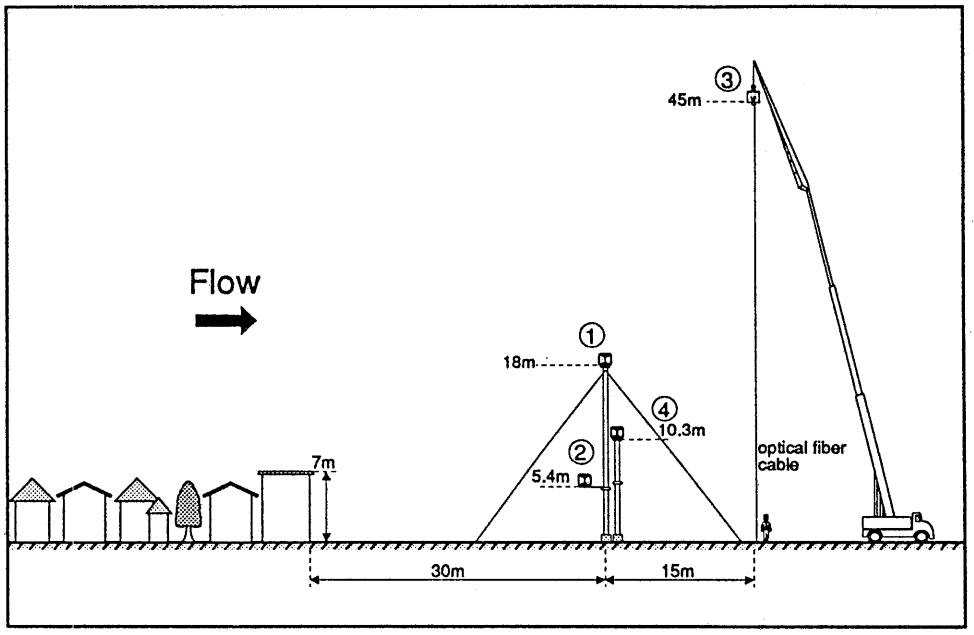

Fig. 2. Schematic of experimental setup. The ultrasonic anemometers of ①, ② and ③ were used in Period A, and those of ①, ② and ④ were used in Period B.

at the end of a 1 m boom extending northeast from the pole. The data reported in this study were measured on two separate occasions. In 1991 (Period A), three ultrasonic anemometer-thermometers were set at heights of 5.4 and 18 m on a pole and 45 m on a mobile crane to measure turbulence characteristics in and above the canopy as a whole. Although ideally the crane-mounted ultrasonic sensor should be set directly over the pole, this would create a hazardous situation in which a fine optical fiber cable could become entangled with the supporting wires and pole. In the present study, to avoid contact between the optical fiber cable and the 18 m pole, the sensor mounted on the mobile crane was set back 15 m from the 18 m pole in the alongwind direction. The result from the preliminary wind tunnel study (1:175 scale model) showed a difference of less than 1% in mean wind speed and the standard deviations of the two wind components between the pole and crane sensor positioned at $z = 45$ m ($z = 25.7$ cm in the wind tunnel). In 1992 (Period B), the three ultrasonic anemometer-thermometers were set up at 5.4, 10.3 and 18 m on the poles to clarify the organized motion near the canopy. To examine the lateral configuration of organized structure, the 10.3 m pole was set at a position with a 18.7 m lateral distance from the 18 m pole. Considering that the upwind terrain was such that it could be regarded as two-dimensional, mean wind speed and turbulence statistics obtained with the two poles at different lateral locations were analyzed as though they were obtained from one position. The result of the preliminary wind tunnel study showed a difference of less than 1% in mean wind speed and turbulence statistics between the two poles positioned at heights of $z = 10.3$ m ($z = 5.8$ cm in the wind tunnel).

TABLE I

Summary of field experiment conditions (values are the average of 9 runs)

Date	z (m)	U (m/s)	σ_u (m/s)	σ_v (m/s)	σ_w (m/s)	u_* (m/s)	$\overline{w'\theta'}$ (m/s · K)	L (m)
Period A July 1991	45.0	3.8	0.72	0.82	0.68	0.41	0.12	−44
	18.0	3.3	0.96	0.91	0.67	0.54	0.17	−68
	5.4	2.3	0.94	0.97	0.61	0.49	0.14	−61
Period B Nov. 1992	18.0	5.7	1.29	1.25	0.76	0.60	0.08	−190
	10.3	3.7	1.49	1.17	0.75	0.64	–	–
	5.4	2.9	1.26	1.13	0.71	0.54	0.06	−185

2.4. Observation Period and Atmospheric Conditions

Period A was conducted from July 9–13, 1991, for a total of 30 hours over five days. From the 9th to the 11th, five hours of data were collected from the ultrasonic anemometer mounted on the mobile crane. Period B measurements were conducted for a total of 22 hours over the period November 11–13, 1992.

Atmospheric conditions and turbulence properties during these two periods are shown in Table I. Here, z is the height above ground, and $z' = z - d$, where d is the zero-plane displacement. The zero-plane displacement d (= 2.3 m) was calculated using the method described by Counihan (1971), where U is the mean horizontal wind speed, and σ_u, σ_v, and σ_w are the standard deviations of the fluctuating velocity components along the alongwind (x), crosswind (y), and vertical (z) directions, respectively. The friction velocity u_* was derived from the eddy correlation measurements, with $u_* = \sqrt{-\overline{u'w'}}$; and L is the Monin–Obukhov stability length, $L = -u_*^3 T_0/\kappa g \overline{w'\theta'}$, where θ' is temperature fluctuation, κ is the von Karman constant (0.41), T_0 is the potential temperature, and g is the acceleration due to gravity. Observations were conducted mainly during daytime on both clear and cloudy days. Atmospheric conditions were slightly unstable, where the values of z'/L at $z = 18$ m were -0.23 and -0.08 for Periods A and B, respectively.

In order to compare observations at different periods, a friction velocity u_{*_r} measured at $z = 18$ m for a reference velocity was defined. This level was little disturbed by the individual roughness elements and represents the roughness sublayer (see Section 3). Table II provides a summary of the data used for the spectral analysis and for investigating the ensemble-averaged image of the organized motion.

TABLE II

Summary of data used for the spectral analysis and for investigating the ensemble-averaged image of the organized motion (at height $z = 18$ m)

Date	Run	Observation period	U (m/s)	u_* (m/s)	$\overline{w'\theta'}$ (m/s · K)	L (m)
Nov. 11, 1992	B01	1325–1335	7.1	0.67	0.08	−250
(Period B)	B02	1345–1355	7.4	0.89	0.10	−478
	B03	1355–1405	6.7	0.58	0.04	−320
	B04	1405–1415	7.2	0.76	0.06	−552
	B05	1433–1443	7.4	0.60	0.03	−515

3. Results of Turbulent Statistical Analysis

3.1. Vertical Profiles of Mean Velocity and Turbulence Statistics

In the wind tunnel, the measurement of turbulence characteristics within and above the canopy is very difficult because of the high intensity of turbulence. The conventional X-wire probe anemometers for turbulence measurement in the wind tunnel cannot give reasonable accuracy when the turbulence intensities are larger than 0.3 (Tutu and Chevray, 1975). Recently, the quality of measurement of $-\overline{u'w'}$ has improved with the use of coplanar triple-wire probes. This type of probe has an acceptance angle close to $\pm 90°$ and performs satisfactorily when σ_u/U is 0.5 or higher (Raupach *et al.*, 1986). A recent review (Raupach, 1989) showed a clear picture of canopy turbulence. The data came from seven different plant canopies: two forests, two corn crops and three wind tunnel model plant canopies. Even though the canopies varied widely, the flow structure had well-deflned features in common. However, very few studies deal with observed turbulence profiles over built-up surfaces.

Figure 3(a) shows mean wind speed profiles, plotted against normalized height z/h ($h = 7$ m, where h is the canopy height). The circles (Period A) and squares (Period B) represent the average of nine runs; the error bars represent the standard error. The two dashed and dotted lines in Figure 3(a) represent non-neutral wind profiles calculated by the equation $U/u_* = (1/\kappa)\{\ln(z'/z_0) - \psi(z'/L)\}$, where $\psi(z'/L)$ is the Monin–Obukhov function, z_0 is the roughness length (=0.45 m) which is assessed using the method described by Lettau (1969), and L is the Monin–Obukhov stability length measured at $z = 18$ m from Periods A and B. The calculated wind profiles appear to display the same tendency as those found in the present study, although the value of U/u_* at $z = 18$ m in Period B was slightly larger than the calculated value. The differences in the data between the two periods can be explained by the disparity in stability.

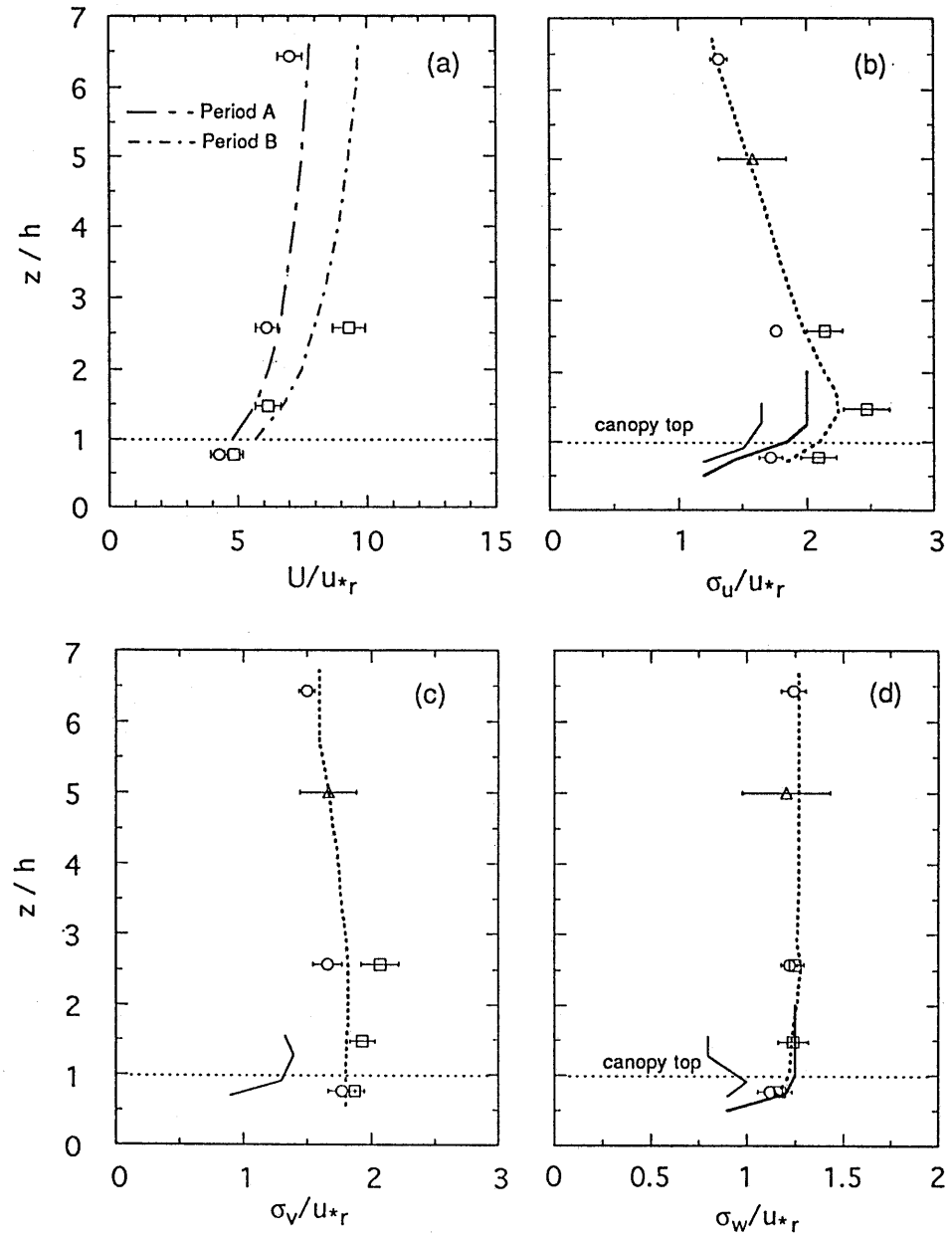

Fig. 3. The profiles of normalized (a) wind speed, (b) σ_u, (c) σ_v and (d) σ_w. The circles (Period A) and squares (Period B) were the average of 9 runs and the triangles (Period A) were the average of 3 runs. The error bars represent the standard error. The dash and dot lines in (a) denoted the mean wind profiles calculated by the equation of $U/u_* = (1/\kappa)\{\ln(z'/z_0) - \psi(z'/L)\}$. In (b)–(d), the dashed curves were drawn by eye, the heavy solid lines represent wind tunnel data (h = 60 mm) from Raupach (1989), and the thin solid lines represent the urban canyon data (h = 18.3 m) from Rotach (1991, 1993a).

Figure 3(b)–3(d) presents vertical profiles of the standard deviation of the velocity components normalized by the friction velocity u_{*_r} at 18 m. The heavy solid lines shown in Figure 3(b)–3(d) represent wind tunnel data (h = 60 mm) from Raupach (1989), and the thin solid lines show urban canyon data (h = 18.3 m)

from Rotach (1991, 1993a) observed in the city center of Zürich, Switzerland. The profiles of velocity fluctuation σ_v and σ_w had nearly uniform profiles; on the other hand, the profiles of σ_u had a broad peak above the canopy and attenuated with height thereafter. The values of σ_w/u_* between Periods A and B agree very well, but the value of σ_u/u_* and σ_v/u_* between both periods did not. The results may be attributable to the fact that the values of σ_u/u_* and σ_v/u_* are generally marked by considerable scatter even in the homogeneous surface layer. Panofsky and Dutton (1984) recommended values of 2.4, 1.9 and 1.25 for σ_u/u_*, σ_v/u_* and σ_w/u_*, respectively, in neutral conditions and flat terrain. The values above the canopy in the present study correspond approximately with these recommended values. The profiles of turbulence observed in the present study also agree with those from wind tunnel studies. However, Rotach's data show lower values. The reason for this difference might be attributable to overestimation of his reference u_{*_r}.

Figure 4 illustrates the Reynolds stress profile normalized by $u_{*_r}^2$. The profile of momentum flux peaked slightly at 1.5 times the canopy height and decreased slowly with height thereafter. The profiles of Reynolds stress measured in the wind tunnel study over the plant canopies indicated a constant value above the canopy, even with a wide range of plant canopy types (Raupach,1989). For comparison, Raupach's wind tunnel data and Rotach's data in an urban canyon are also shown in this figure as a heavy solid line and a thin solid line, respectively. In the present study, Reynolds stress had a value similar to Raupach's results. However, the data observed by Rotach show lower values compared to the present data and other canopy data. This may be attributable to the use of his reference u_{*_r} (at $z/h = 2.07$, $z = 38$ m), which was not measured directly and was estimated from the equation $u_{*_r} = \kappa z'(\mathrm{d}U/\mathrm{d}z')/(\Phi_m(z'/L))$, where $\Phi_m(z'/L)$ is the semi-empirical function for dimensionless wind shear. In this equation, the gradient of the mean wind speed was computed by the data at the end of the measured wind profiles. Since the wind velocity field on the roof was strongly influenced by buildings, the reference u_{*_r} may not be correctly estimated using this equation. It is highly possible that u_{*_r} was overestimated, especially considering that the data were shifted towards lower values compared to the present data and other canopy data. Rotach concluded that the Reynolds stress values in an urban roughness sublayer increased with height when based on the measurement height range of about 1.5 times the canopy height. However, this conclusion should be applicable only near the canopy.

3.2. Normalized Velocity and Temperature Fluctuations

According to Monin–Obukhov similarity theory, the normalized standard deviation of velocity and temperature fluctuations within the surface layer can be described as a function of (z/L):

$$\sigma_{u,v,w}/u_* = f_{u,v,w}(z/L), \quad \sigma_\theta/T_* = f_\theta(z/L) \tag{1}$$

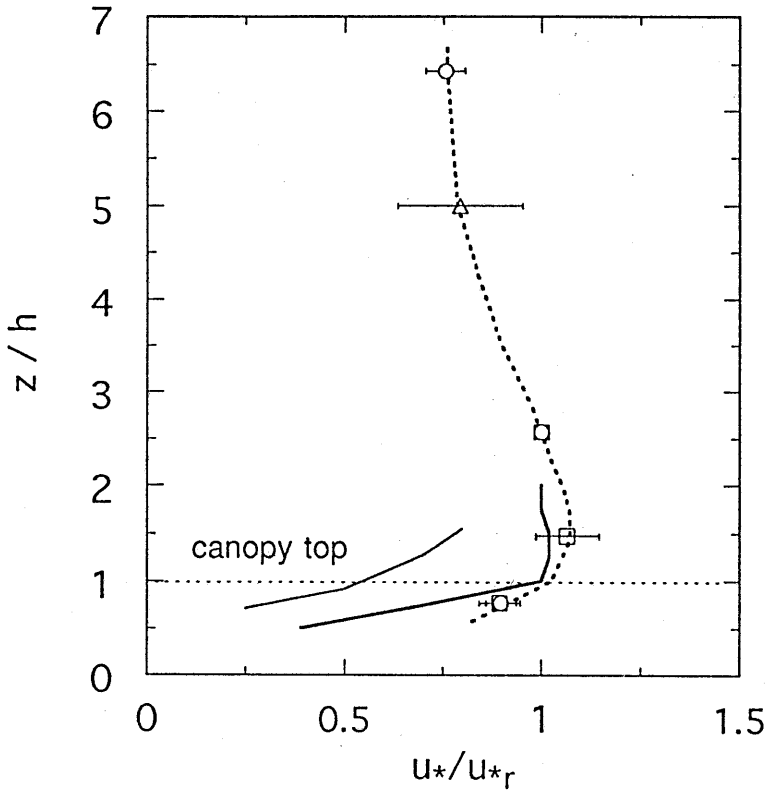

Fig. 4. The normalized Reynolds stress profiles. The dashed curve was drawn by eye. The details of the symbols and the line follow Figure 3(b)–(d).

where $f_{\underline{u,v,w},\theta}(z/L)$ are the corresponding universal similarity functions, and $T_* = -\overline{w'\theta'}/u_*$ is the friction temperature. Though the Monin–Obukhov similarity theory is only applicable in the homogeneous surface layer, it is also used in the roughness sublayer because of the absence of a suitable framework.

Figure 5 shows the normalized standard deviation of the velocity and temperature fluctuations from near-neutral to unstable conditions. In this figure, u_* and L are taken as local values, in light of the suggestion by Högström *et al.* (1982) that local scaling was appropriate for the urban roughness sublayer. The data of σ_u/u_* and σ_v/u_* above the canopy, at $z = 18$ m, are found to be close to the $(-z'/L)^{1/3}$ similarity prediction for $-z'/L > 0.4$ with considerable scatter, as observed by Steyn (1982) and Roth (1993). Within the canopy, at $z = 5.4$ m, the same tendency was found as that at $z = 18$ m, but the trend was obscure because of a lack of data at the large instability value. The values of σ_v/u_* at $z = 18$ m were slightly lower than the relationship for an urban site (Ar/A = 25%, $h = 5.5$ m, $z = 31$ m) predicted by Clarke *et al.* (1982), while the values of σ_v/u_* at $z = 5.4$ m were slightly higher than those found by Clarke *et al.*

The σ_w/u_* data within and above the canopy (Figure 5(c)) corresponded closely to $(-z'/L)^{1/3}$ for $-z'/L > 0.3$ as predicted by the similarity theory, and their magnitudes were slightly higher than the values reported by Clarke *et al.* The

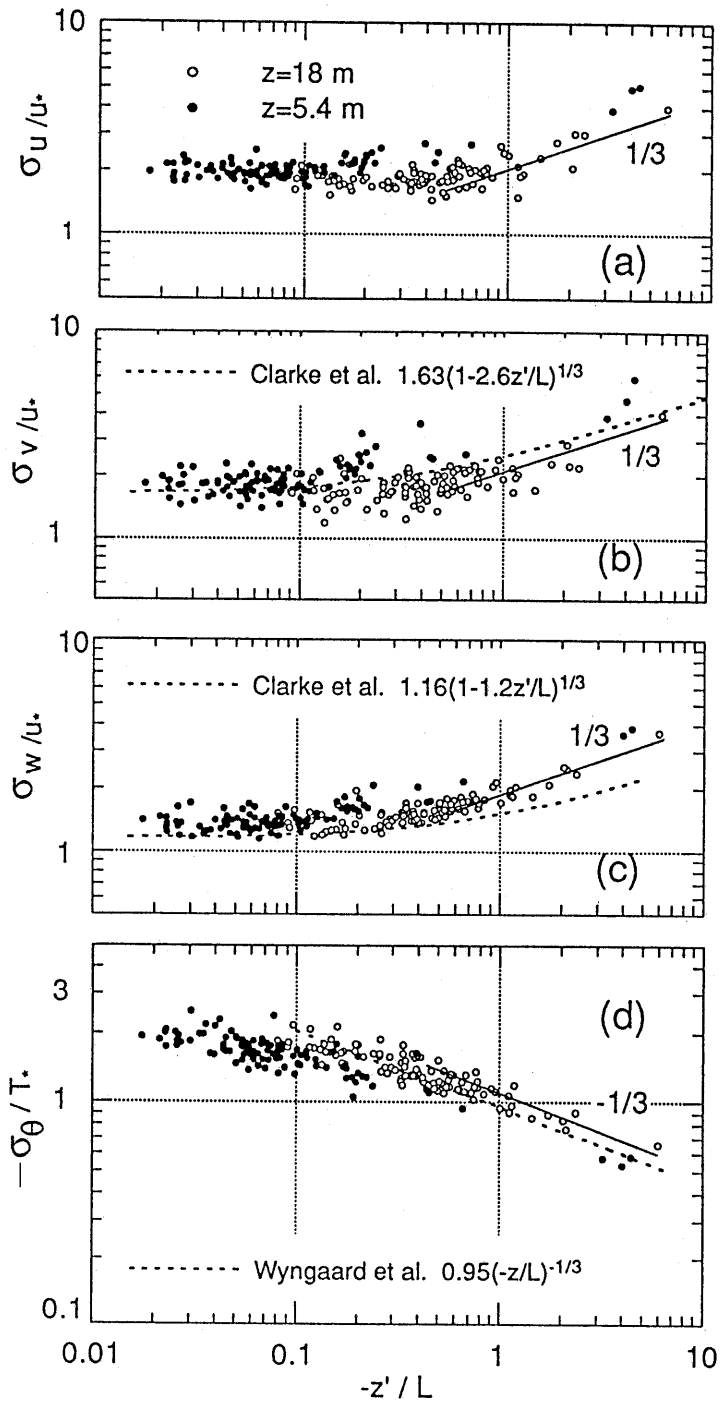

Fig. 5. Normalized velocity and temperature fluctuations under unstable conditions (100 runs in Period A). The solid lines represent the predicted slope of Monin-Obukhov similarity. (a) longitudinal velocity fluctuations (b) lateral velocity fluctuations (c) vertical velocity fluctuations (d) temperature fluctuations.

σ_w/u_* data above the canopy were slightly smaller than within the canopy, as observed in Rotach's study (1993b) above a street canyon. He found that the σ_w/u_* data at $z = 28$ m were lower than those at $z = 23$ m. Extrapolating the

σ_w/u_* data to $z'/L = 0$ results in a value of approximately 1.3 at $z = 18$ m and 1.4 at $z = 5.4$ m, in satisfactory agreement with most suburban and urban observations (e.g., Bowne and Ball, 1970:1.3; Högström *et al.*, 1982: 1.5; Clarke *et al.*, 1982: 1.2; Roth, 1993: 1.2).

The slope of σ_θ/T_* within and above the canopy (Figure 5(d)) was approximately proportional to $(-z'/L)^{-1/3}$ for $-z'/L > 0.4$, as predicted by similarity theory. The values of σ_θ/T_* at $z = 18$ m were slightly higher than those observed by Wyngard *et al.* (1971) for a uniform fetch and Roth (1993) for a suburban site.

As mentioned above, the normalized standard deviation of three fluctuating velocity components and the temperature fluctuations above and within the canopy correspond approximately to the predicted slope of Monin–Obukhov similarity theory under unstable conditions. The magnitudes of the normalized standard deviation of the three velocity fluctuations above the canopy (at $z = 18$ m) were systematically smaller than those within the canopy (at $z = 5.4$ m), while temperature fluctuation data above the canopy were higher than within the canopy.

3.3. Energy Spectra

Spectral data obtained in the roughness sublayer are very limited in the literature. The urban and suburban data at a more elevated height, obtained by Högström *et al.* (1982), Clarke *et al.* (1982), and Roth and Oke (1993), differ slightly from those obtained over an ideal surface. In this study, the power spectra of velocity components (u, w) were calculated by the Fast-Fourier Transform (FFT) method using consecutive 4096 data points. The spectral plots were smoothed by the block-averaging method proposed by Kaimal and Gaynor (1983). In order to reduce the influence of aliasing, the several highest frequencies were not included in the analysis. Figure 6 shows normalized spectra against a non-dimensional frequency $f = nz'/U$ (where n is the natural frequency in Hz) of the longitudinal and vertical velocity components for an average of five runs (B01–B05). The suburban results shown in the figures are those of Roth and Oke (1993) in Vancouver (at $z' = 19$ m).

The u spectra at heights of 5.4 and 18 m are shown in Figure 6(a). A $-2/3$ slope in the inertial subrange, predicted by Kolmogorov's hypothesis, was almost attained. Comparing the reference data, however, the data at 18 m shifted slightly to the lower frequency range. Above the canopy, at $z = 18$ m, the highest spectrum value was found at about $f = 0.04$, with a possible range of $f = 0.01 \sim 0.05$, and a prominent dip at $f = 0.06$. Although within the canopy, at $z = 5.4$ m, the dip at the low frequency range made determination of a peak frequency difficult, the u spectra had a broad peak in the range $f = 0.01 \sim 0.05$.

The w spectra at heights of 5.4 and 18 m (Figure 6(b)) correspond approximately to the $-2/3$ slope in the inertial subrange. At $z = 18$ m, the peak of the w spectrum was broadened at the range of $f = 0.1 \sim 0.4$, and a prominent dip appeared at

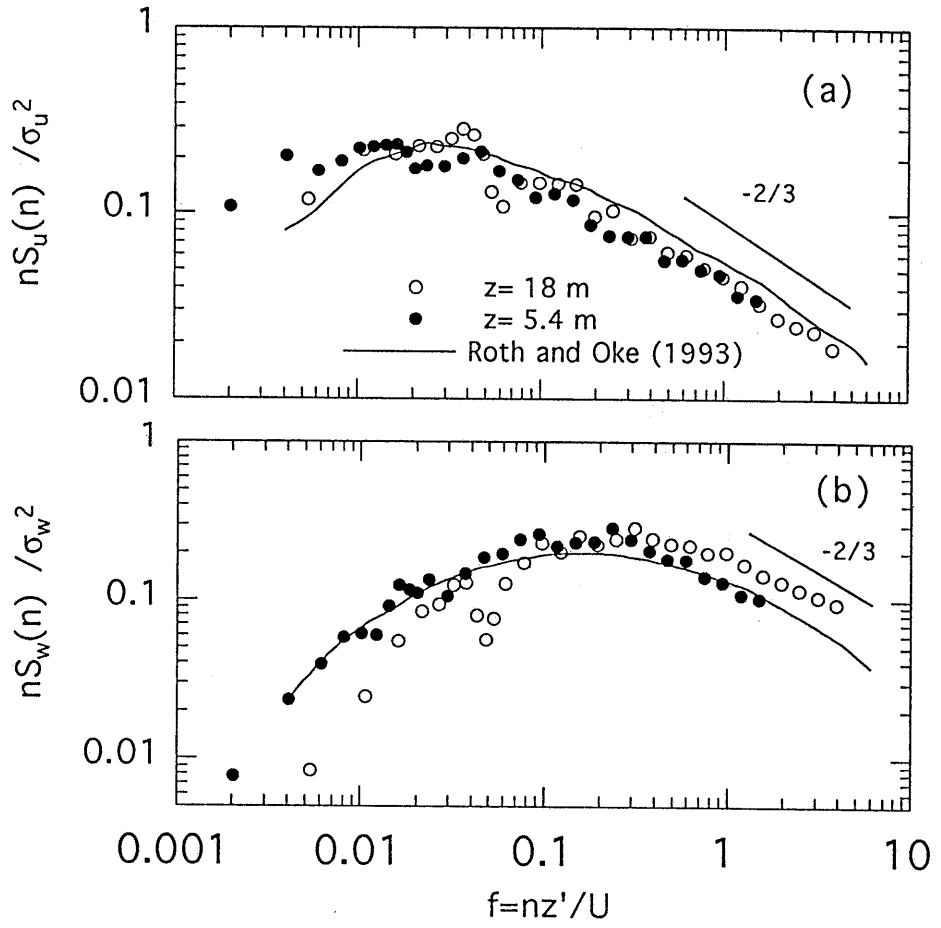

Fig. 6. The normalized spectra of (a) u and (b) w for the average of Runs B01–B05. The lines are data from Roth and Oke (1993).

$f = 0.05$. The peak of the w spectrum at $z = 5.4$ m appeared in the range of $f = 0.08 \sim 0.3$. The shape of the w spectrum at $z = 5.4$ m was similar to that of the reference curve, while the shape at $z = 18$ m appears to shift slightly towards a higher frequency region in comparison to the reference curve. Note that the w spectra at $z = 18$ m had a dip at approximately the same frequency as that found for the u spectrum.

The dips appearing in the range $f = 0.05 \sim 0.06$ in the present study were approximately equivalent to $n = 0.02$ Hz, which in turn gave a period of $T = 1/n = 50$ s. This frequency (0.02 Hz) was lower than the natural frequency (0.18 Hz) of the mast calculated using the cantilevered model with a lumped mass at the tip. This indicates that the supporting system did not contribute to the dip. In fact, the frequency of dips nearly corresponded to the frequency of production of the larger Reynolds stress generated by the sweep and ejection motions (see Figure 8), implying that these dips may be related to organized motions. Spectra at comparable heights over the roughness sublayer are very limited in the literature. Rotach's study (1991) at a small elevation z/h (=1.27) above a street canyon

showed a pronounced dip at $f = 0.04$ in the u-spectra, which was similar to that found in the present study.

4. Organized Motion

4.1. Quadrant Analysis

Organized structures have been identified and studied in various turbulent flow conditions (Kline *et al.*, 1967; Grass, 1971; Antonia *et al.*, 1979; Gao *et al.*, 1989), and various quantitative methods for identification of turbulent structures have been developed. One of these is quadrant analysis (Wallace *et al.*, 1972; Lu and Willmarth, 1973). In quadrant analysis, $u'w'$ is divided into four different quadrants. Quadrants two and four, representing ejection and sweep, respectively, make positive contributions to the Reynolds stress, while quadrants one and three make negative contributions.

In a laboratory study, Nakagawa and Nezu (1977) recorded several significant findings using open-channel water flow over glass bead roughness. They found that sweep events were more important than ejection events for momentum transfer close to a rough wall, and also that the sweep-to-ejection ratio increased with decreasing height and increasing roughness. In a vegetated canopy, Finnigan (1979) observed that ejection was negligible within the canopy of a uniform wheat crop but that ejection began to increase above the canopy. However, with the exception of Rotach (1993a), few observations have been made of sweep and ejection events in an urban canopy.

Figure 7 shows the time variation of velocity fluctuations u', w', the instantaneous Reynolds stress $-u'w'$, and the temperature fluctuation θ' at the 5.4 and 18 m heights. Run (B02) was conducted from 1345 to 1355 JST in November 1992 under slightly unstable conditions ($L = -478$ m at $z = 18$ m). The plots were smoothed by a 1-s running average. The positive instantaneous Reynolds stress $-u'w' > 0$ occurred at almost the same time at the 5.4 and 18 m levels. In the sweep event ($u' > 0, w' < 0$), high-velocity fluid from above moved downward towards the surface, and cold air swept down from above the canopy, causing a negative temperature fluctuation. Conversely, in the ejection event ($u' < 0, w' > 0$), low-velocity fluid from below moved upward, and warm air ejected up from the canopy caused a positive temperature fluctuation. Figure 8 shows the data at 18 m smoothed by a long running average. The sweep and ejection events occurred periodically at 100 s intervals.

A stress fraction, S_i, which is the conditionally averaged stress $-\langle u'w' \rangle_i$ in i quadrant normalized by the total mean averaged Reynolds stress $-\overline{u'w'}$, is defined in the equation $S_i = \langle u'w' \rangle_i / \overline{u'w'}$. Figure 9 shows the relationship between the skewnesses ($Sk(u) = \overline{u'^3}/\sigma_u^3$, $Sk(w) = \overline{w'^3}/\sigma_w^3$) and the difference $\Delta S (= S_4 - S_2)$ between sweep and ejections fractions for 100 runs at $z = 5.4$ and 18 m.

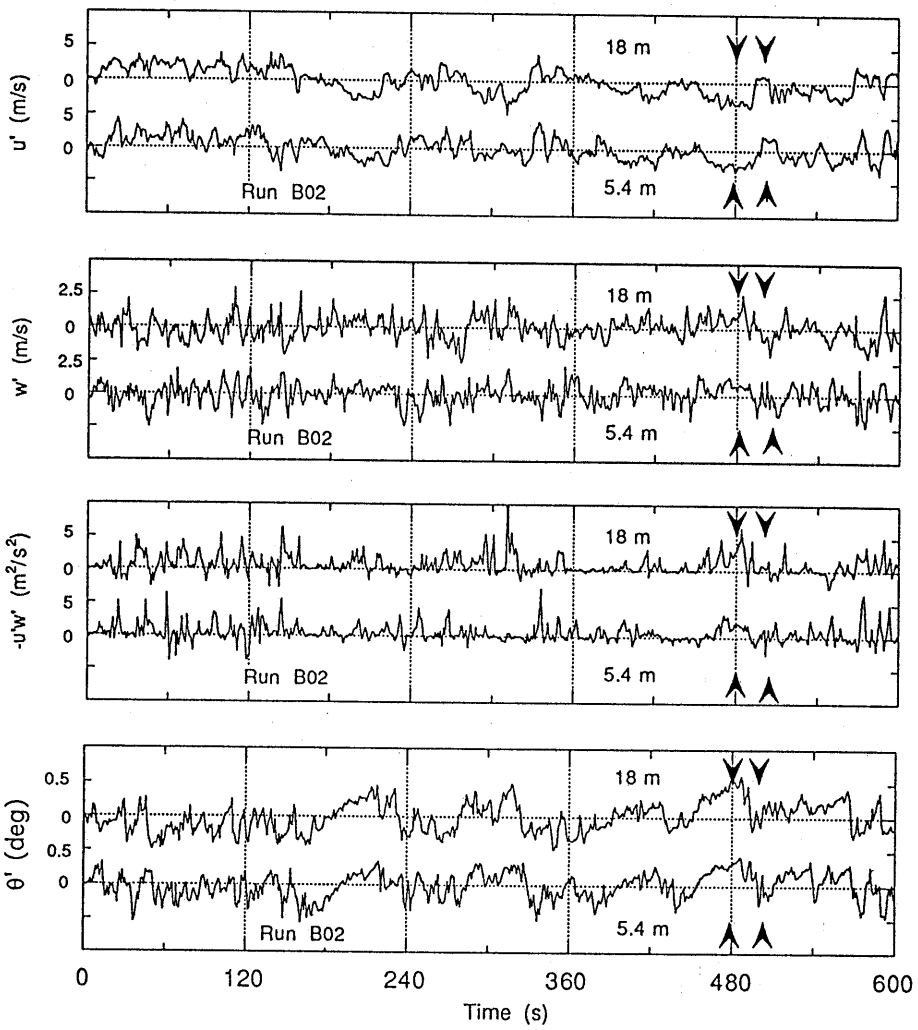

Fig. 7. Time series of fluctuating u', w', $-u'w'$ and θ' at 18 and 5.4 m heights during 10 min of Run B02. The arrows show sweep and ejection motions.

Occurrences of ejection appear much greater than of sweep above the canopy, while in the canopy, occurrences of sweep appear greater than ejection. It was found that the skewness is approximately proportional to ΔS. This suggests that a skewed distribution of the longitudinal and vertical velocity components resulted from sweep and ejection motions.

Figure 10(a) illustrates the profiles of $-\langle u'w'\rangle_i/u_{*_r}^2$, which were averaged in Periods A and B. The values of the sweep and ejection events, which make a positive contribution to the Reynolds stress, were larger than the interaction events. It is obvious that both of these typical motions above the canopy caused the higher layer of Reynolds stress. This result helps to explain the process of generation of Reynolds stress near the canopy. Figure 10(b) shows a ratio of S_4/S_2 for momentum transfer by sweeps to that by ejections. The heavy and thin solid lines represent wind tunnel data (h = 60 mm) from Raupach (1989) and urban

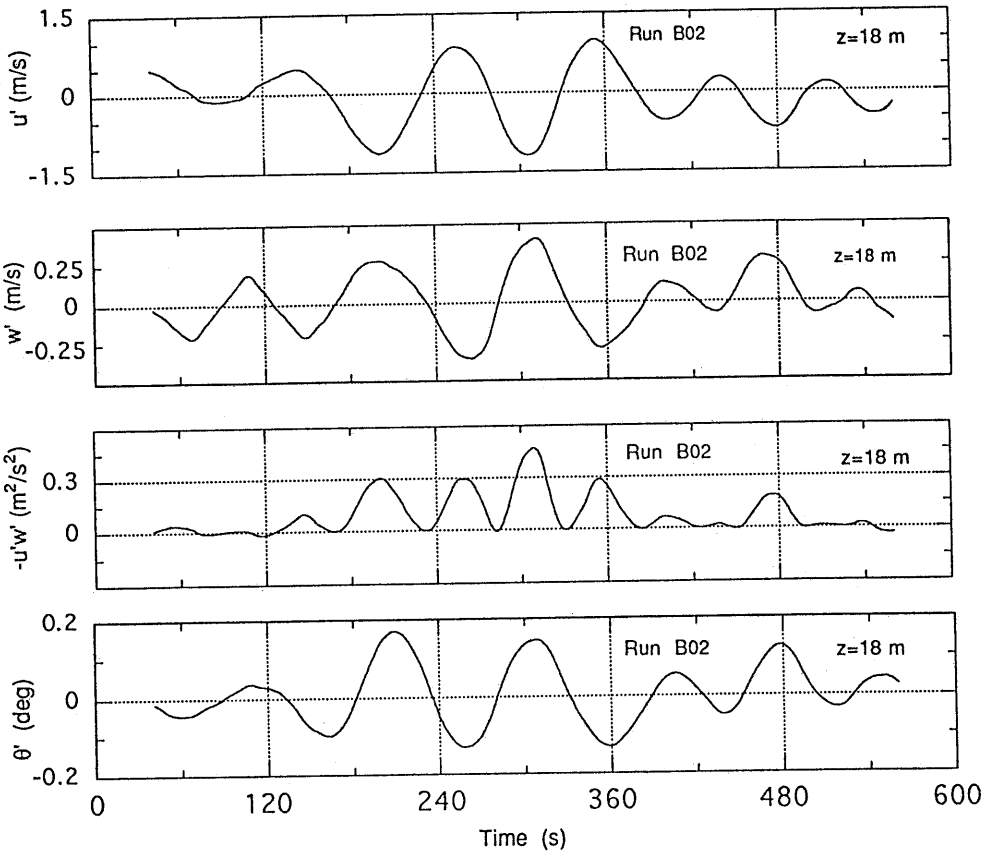

Fig. 8. The smoothed u', w', $-u'w'$ and θ' data at $z = 18$ m for Run B02.

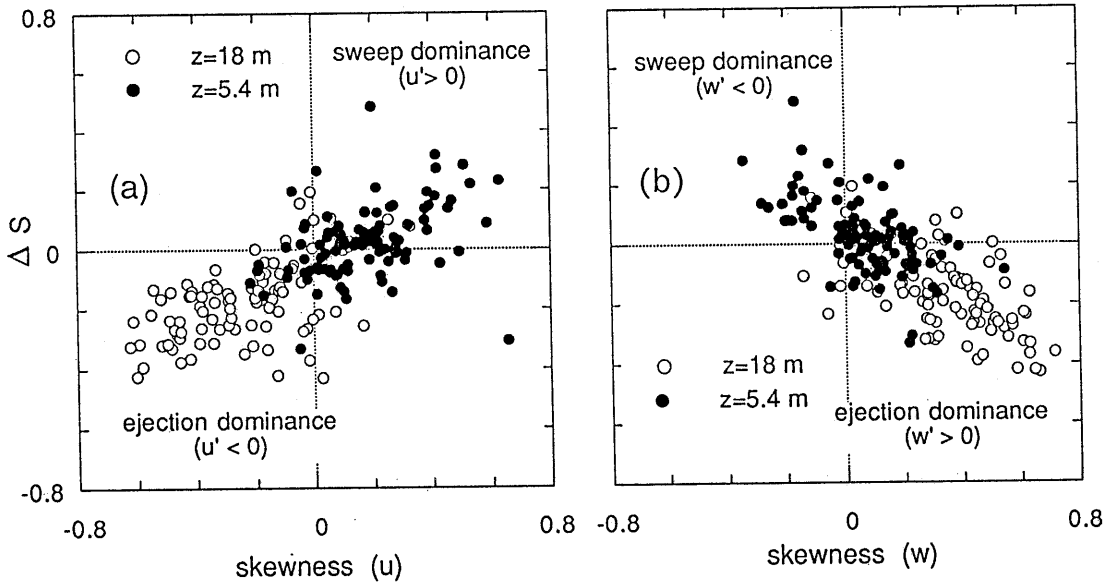

Fig. 9. Relationship between skewness and the difference ΔS between stress fractions due to sweeps and ejections (100 runs in Period A) (a) longitudinal velocity (b) vertical velocity.

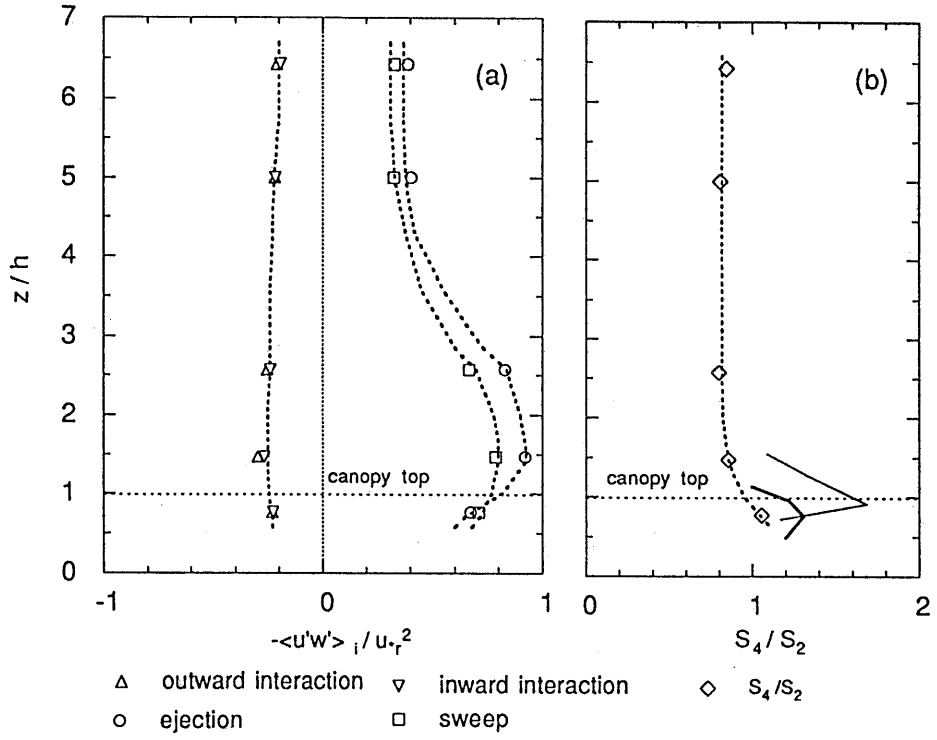

Fig. 10. The profiles of (a) the conditionally averaged Reynolds stress normalized by $u_{*_r}^2$ measured at $z = 18$ m and (b) the sweep-to-ejection ratio S_4/S_2. The data of at 5.4 and 18 m are averages of Periods A and B. The dashed curves were drawn by eye. In (b), the heavy and thin solid lines represent wind tunnel data ($h = 60$ mm) from Raupach (1989), and the urban canyon data ($h = 18.3$ m) from Rotach (1993a).

canyon data ($h = 18.3$ m) from Rotach (1993a), respectively. The ratio S_4/S_2 generally decreased with increasing height. The data in the present study near the canopy were found to be close to the data found in rough-wall wind tunnel studies.

The height of the roughness sublayer, z_*, depends on the roughness elements and their spatial distribution: z_* can be described in terms of h (canopy height), D (the separation distance of roughness elements) and z_0 (the roughness length). A wind tunnel study (Raupach *et al.*, 1980) showed that $z_* = h + 1.5D$, and field studies above plant canopies showed $z_* = 3 \sim 4.5h$ (Garratt, 1978) or $z_* = 35 \sim 150\, z_0$ (Garratt, 1980). However, there have not been any observations performed at the height of the roughness sublayer in an urban canopy. In the present study, profiles of sweep and ejection show that an upper height limit of organized motion exists at about 3–4 h, when based upon the momentum flux attenuating with a height of about 30 m thereafter. It is believed that this height is equivalent to the upper height limit of the roughness sublayer in which roughness elements, such as buildings and trees, have a direct influence on the flow.

4.2. Flow and Temperature Fields of Ramp Structure

A typical temperature ramp feature is characterized by a gradual rise in temperature followed by a relatively sudden drop. Antonia *et al.* (1979) concluded that ramp-jump temperature structures should be interpreted as the signature of organized, large-scale, shear-driven motion, rather than as a result of the buoyancy field. Direct observations of ramp structures for velocity or temperature fields within and above vegetated canopies were obtained by Bergström and Högström (1989) and Gao *et al.* (1989). The data obtained by Gao *et al.* (1989) revealed periods when a large number of ramp patterns appeared repeatedly in the time series of temperature and humidity. The ramps occurred at nearly the same time at several levels both within and above the canopy. Flow fields associated with these ramps, displayed by a time-height cross-section of scalar contours and velocity vectors, showed strong organization. However, there are no observations of temperature ramps in an urban roughness sublayer. In the present study, data from sonic anemometers in and above the canopy were analyzed in a manner similar to that of Gao *et al.* (1989).

An example of ramp events is shown in Figure 7 (at a range between 440 and 500 s). The temperature variation follows distinct ramp patterns characterized by a gradual rise and terminated by a sharp drop of about 0.8 °C over 1 to 3 s. The ramps occur nearly simultaneously at the 5.4 and 18 m levels. The ensemble-averaging technique was used to isolate typical features of the flow and temperature fields for a relatively large number of events in and above the urban canopy. An instantaneous quantity, S, in the flow is decomposed into a mean or synoptic value $\bar{S}$, a large-scale component including ramp events $\tilde{s}$, and a high-frequency random turbulent component s'' in the triple decomposition scheme proposed by Reynolds and Hussain (1972), as

$$S = \bar{S} + s' = \bar{S} + \tilde{s} + s''. \tag{2}$$

Following Gao *et al.* (1989), the synoptic values were removed by subtracting a 10-min running average of the wind and temperature components. By ensemble averaging of a number of ramps, the effect of smaller scale random turbulence was diminished and the organized motions more easily seen. First, the individual ramp events were subjectively identified in the rapid temperature drop at the 18 m height. Next, the temperature and velocity data, centered on the sharp temperature decrease, were recorded at all levels and averaged. No attempt was made to adjust time scales to match ramps of different duration. Analysis was performed on a total of 10 ramp events during a 40-min period (Runs B02–B05).

Figure 11 shows an example of the ensemble-averaged $\tilde{u}$, $\tilde{w}$ and $\tilde{\theta}$ derived from 10 sampling data sets. The ramp is associated with velocity fields; that is, an upward vertical velocity is generally found in the interior of the ramp, while the surrounding area is dominated by downward motion. The horizontal scale of the organized motion was approximately 380 m, calculated from the period of organized motion (80 s) and wind speed (4.8 m/s) at 10.3 m. The ramp downdraft

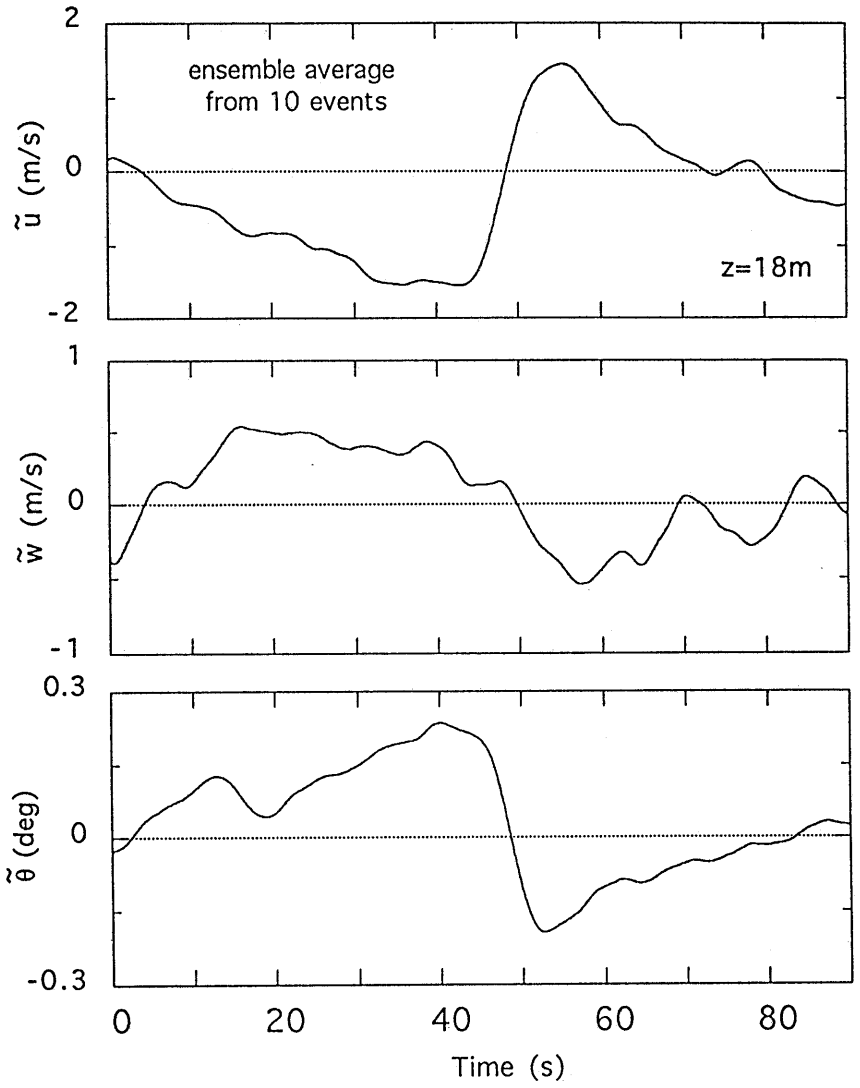

Fig. 11. Ensemble-averaged $\tilde{u}$, $\tilde{w}$ and $\tilde{\theta}$ at $z = 18$ m derived from 10 sampling data sets.

length in this case was approximately half that of the horizontal scale of the organized motion (190 m). Bergström and Högström (1989) observed organized motions above a forest ($h = 20$ m) and estimated the ramp downdraft length in the range 38 to 1012 m, with a mean value of 238 m. This horizontal scale appears to agree in order of magnitude with the horizontal scale (190 m) observed in the present study.

Figure 12 shows the ensemble-averaged fluctuating $\tilde{u}$, $\tilde{w}$ velocity and temperature fields at 5.4, 10.3 and 18 m. The velocity vectors are plotted in the $(-t, z)$ plane and the data at 10.3 m are shown by dotted arrows because the data were obtained at a location different from that of the other two ultrasonic anemometers. With the frozen-field approximation, the $-t$ horizontal axis corresponds to the $+x$ axis, so the ensemble-averaged image of organized motions in the xz-plane can be seen in

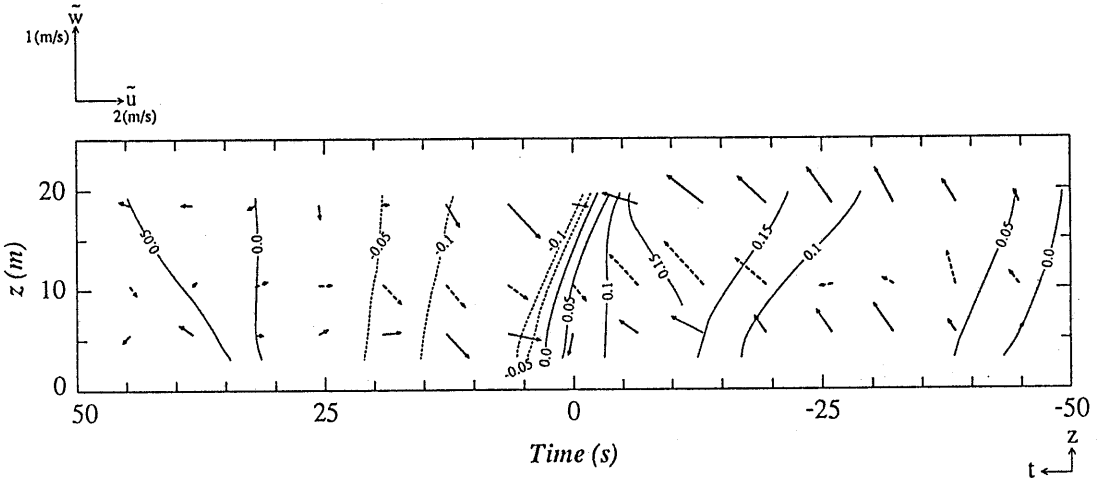

Fig. 12. The vertical cross-section of the ensemble-averaged fluctuating velocity and temperature fields from 10 events. The data at 10.3 m are shown by the dotted arrows. Solid and dashed lines indicate isotherms above and below the mean. Contour interval is 0.05°C.

this figure. Although the 10.3 m mast was positioned at a 18.7 m lateral distance from the 18 m mast, the time series observed at the two positions showed strong correlation. The sweep and ejection motions occurred at almost the same time, and the space correlation coefficient was 0.8 for longitudinal velocity fluctuations (20 s running average) at 18 and 10.3 m. The result implies that the organized structure near the urban canopy has a lateral expansion.

The formation mechanism of organized structure in and above the canopy was explained by Raupach *et al.* (1989); that is, organized structure generated in and above the canopy was induced by an inflection point instability of the velocity profile because of the canopy. Recently, Kanda and Hino (1994) used a large eddy simulation model to calculate the turbulent flow within and above a plant canopy. They also suggested that the organized structures generated at the boundary were induced by the shear instability at inflection points of the velocity profile.

The temperature contours superimposed on the velocity vector field are shown in Figure 12. Dashed and solid lines show isotherms below and above the mean value, respectively, at contour intervals of 0.05 °C. The shift in the sign of vertical velocity occurs almost simultaneously within and above the canopy, in contrast with the passage of the thermal microfront. A zero line separates the field into regions of updraft and downdraft, in which appear positive and negative temperature fluctuations, respectively. As a result, a positive heat flux was created, and the temperature field was made uniform. It is clear that the organized motion found in the present study plays an important role in the transport of heat in and above the urban canopy, where the sweep motion caused a negative temperature fluctuation and the ejection motion caused a positive temperature fluctuation.

In general, an urban atmosphere does not experience a strong diurnal change in stability, because a well-mixed urban layer tends to destroy strong temperature

gradients (Oke, 1987). In the present study, an unstable condition in the upper layer above the canopy ($z'/L = -0.97$ at $z = 45$ m) was observed but, near the canopy, slightly unstable and near-neutral conditions ($z'/L = -0.23$ at $z = 18$ m; $z'/L = -0.05$ at $z = 5.4$ m) were observed. Decreasing unstable conditions with decreasing height in an urban atmosphere can be explained by mechanical mixing caused by the organized motions.

5. Summary

Turbulent properties and organized motions in a suburban roughness sublayer were observed during a field study performed in Sapporo, Japan. It was found that:

(1) The profiles of σ_u had a broad peak above the canopy, while σ_v and σ_w had nearly uniform profiles. Vertical profiles of Reynolds stress, $-\overline{u'w'}$, peaked slightly at 1.5 times the canopy height and decreased slowly with height thereafter.

(2) The normalized standard deviation of three fluctuating velocity components and the temperature fluctuation above and within the canopy correspond approximately to the predicted slope of the Monin–Obukhov similarity theory under unstable conditions. The magnitudes of the normalized standard deviation of the three velocity fluctuations above the canopy (at $z = 18$ m) were systematically smaller than those within the canopy (at $z = 5.4$ m), while temperature fluctuation data above the canopy were higher than those within the canopy.

(3) The u and w spectra at heights of 5.4 and 18 m showed that the $-2/3$ slope in the inertial subrange, predicted by Kolmogorov's hypothesis, was almost attained. The peaks of the u and w spectra within and above the canopy were broadened in the range of $f = 0.01 \sim 0.05$ and $f = 0.08 \sim 0.4$, respectively.

(4) Using a four-quadrant analysis, it was found that the higher layer of Reynolds stress above the canopy was caused by sweep events ($u' > 0, w' < 0$) in which high-velocity fluid from above moves downward towards the surface, and by ejection events ($u' < 0, w' > 0$) in which low-velocity fluid from below moves upward.

(5) A time-height cross-section of the velocity vectors and the temperature contours, obtained by using an ensemble-averaging technique, showed details of the flow structures associated with the temperature ramps. The result demonstrates that the shift in the sign of vertical velocity occurs almost simultaneously within and above the canopy, in contrast with the passage of the thermal microfront. There is a sweep motion behind the microfront and an ejection motion ahead of it. The updraft and downdraft motions caused by the organized motion play important roles in the transport of heat near the urban canopy, where the sweep motion causes negative temperature fluctuations and the ejection motion causes positive ones.

Acknowledgments

The authors wish to express their thanks to Dr. S. Wakamatu, Mr. K. Uehara and Dr. I. Uno of National Institute for Environmental Studies, Japan for their cooperation in the field studies and their discussions and to Dr. P. Diosey-Ogawa of Malcolm Pirnie Inc. for her helpful discussions and corrections of this paper. The authors also would like to thank T. Tomabechi, Assistant Professor at the Hokkaido Institute of Technology, for his assistance during this project.

References

Antonia, R. A., Chambers, A. J., Friehe, C. A., and Van Atta, C. W.: 1979, 'Temperature Ramps in the Atmospheric Surface Layer', *J. Atmos. Sci.* **36**, 99–108.

Bergström, H., and Högström, U.: 1989, 'Turbulent Exchange above a Pine Forest. II. Organized Structures', *Boundary-Layer Meteorol.* **49**, 231–263.

Bowne, N. E. and Ball, J. T.: 1970, 'Observational Comparison of Rural and Urban Boundary Layer Turbulence', *J. Applied Meteorol.* **9**, 862–873.

Brook, R. R.: 1972, 'The Measurement of Turbulence in a City Environment', *J. Applied Meteorol.* **11**, 443–450.

Clarke, J. F., Ching, J. K. S., and Godowich, J. M.: 1982, 'An Experimental Study of Turbulence in an Urban Environment', EPA-600/3-82-062, 167 pp.

Counihan, J.: 1971, 'Wind Tunnel Determination of the Roughness Length as a Function of the Fetch and Density of Three-dimensional Roughness Elements', *Atmos. Environ.* **5**, 637–642.

Duckworth, F. S. and Sandberg, J. S.: 1954, 'The Effect of Cities upon Horizontal and Vertical Temperature Gradient', *Bull. Am. Meteorol. Soc.* **35**, 198–207.

Finnigan, J. J.: 1979, 'Turbulence in Waving Wheat. II Structure of Momentum Transfer', *Boundary-Layer Meteorol.* **16**, 213–236.

Gao, W., Shaw, R. H., and Paw, U. K. T.: 1989, 'Observation of Organized Structure in Turbulent Flow within and above a Forest Canopy', *Boundary-Layer Meteorol.* **47**, 349–377.

Garratt, J. R.: 1978, 'Flux Profile Relations above Tall Vegetation', *Ouart. J. Roy. Meteorol. Soc.* **104**, 199–211.

Garratt, J. R.: 1980, 'Surface Influence upon Vertical Profiles in the Atmospheric Near-Surface Layer', *Quart. J. Roy. Meteorol. Soc.* **106**, 803–819.

Graham, I. J.: 1968, 'An Analysis of Turbulence Statistics at Fort Wayne, Indiana', *J. Applied Meteorol.* **7**, 90–93.

Grant, A. L. M. and Watkins, R. D.: 1989, 'Errors in Turbulence Measurements with a Sonic Anemometer', *Boundary-Layer Meteorol.* **46**, 181–194.

Grass, A. J.: 1971, 'Structural Features of Turbulent Flow over Smooth and Rough Boundaries', *J. Fluid Mech.* **50**, 233–255.

Högström, U., Bergström, H., and Alexandersson, H.: 1982, 'Turbulence Characteristics in a Near Neutrally Stratified Urban Atmosphere', *Boundary-Layer Meteorol.* **23**, 449–472.

Hanafusa, T., Fujitani, T., Kobori, Y., and Mitsuta, Y.: 1982, 'A New Type Sonic Anemometer-Thermometer for Field Operation', *Pap. Meteorol. Geophys.* **33**, 1–19.

Hanafusa, T., Fujitani, T., Kobori, Y., and Yoshida, M.: 1983, 'Wind Measurement by a Strong Wind-Type of Three Sonic Anemometer-Thermometers', *Annual Meeting of Japan Society of Meteorol.* Autumn, P99 (in Japanese).

Jackson, P. S.: 1978, 'Wind Structure Near a City Center', *Boundary-Layer Meteorol.* **15**, 323–340.

Kanda, M. and Hino, M.: 1994, 'Organized Structures Developing Turbulent Flow within and above a Plant Canopy, using a Large Eddy Simulation', *Boundary-Layer Meteorol.* **68**, 237–257.

Kaimal, J. C. and Gaynor, J. E.: 1983, 'The Boulder Atmospheric Observatory', *J. Climate Appl. Meteorl.* **22**, 863–880.

Kline, S. J., Reynolds, W. C., Schraub, F. A., and Rundstadler, P. W.: 1967, 'The Structure of Turbulent Boundary Layers', *J. Fluid Mech.* **30**, 741–773.

Lettau, H.: 1969, 'Note on Aerodynamic Roughness-Parameter Estimation on the Basic of Roughness-Element Description', *J. Applied Meteorol.* **8**, 828–832.

Lu, S. S. and Willmarth, W. W.: 1973, 'Measurements of the Structure of the Reynolds Stress in a Turbulent Boundary Layer', *J. Fluid Mech.* **60**, 481–511.

Meng, Y., Oikawa, S., and Wakamatsu, S.: 1993, 'Coherent Structure in and above the Urban Canopy', *Proc. 25th Conf. on Turbulence, Japan. Soc. Fluid Mech.* 47–50 (in Japanese).

Nakagawa, H. and Nezu, I.: 1977, 'Prediction of the Contributions to the Reynolds Stress from Bursting Events in Open-channel Flows', *J. Fluid Mech.* **80**, 99–128.

Ogawa, Y. and Ohara, T.: 1982, 'Observation of the Turbulent Structure in the Planetary Boundary Layer with a Kytoon-mounted Ultrasonic Anemometer System', *Boundary-Layer Meteorol.* **22**, 123–131.

Ogawa,Y., Ohara, T., Wakamatsu, S., Diosey, P.G., and Uno, I.,: 1986, 'Observation of Lake Breeze Penetration and Subsequent Development of the Thermal Internal Boundary Layer for the Nanticoke II Shoreline Diffusion Experiment', *Boundary-Layer Meteorol.* **35**, 207–230.

Ohara,T., Uno, I., and Wakamatsu,S.: 1989, 'Observed Structure of a Land Breeze Head in the Tokyo Metropolitan Area', *J. Applied Meteorol.* **28**, 693–704.

Oikawa, S.: 1993, 'Vertical Turbulence Structure in and above the Urban Canopy', *J. Japan Society of Air Pollution*, **28**, 348–358 (in Japanese).

Oke, T. R.: 1976, 'The Distinction between Canopy and Boundary-Layer Urban Heat Island', *Atmosphere* **14**, 269–277.

Oke, T. R.: 1987, 'Boundary Layer Climates', Routledge, 435 pp.

Panofsky, H. A. and Dutton, J. A.: 1984, 'Atmospheric Turbulence', J. Wiley, New York, 397 pp.

Raupach, M. R., Thom, A. S., and Edwards, I.: 1980, 'A Wind-tunnel Study of Turbulent Flow Close to Regularly Arranged Rough Surfaces', *Boundary-Layer Meteorol.* **18**, 373–397.

Raupach, M. R., Coppin, P. A., and Legg, B. J.: 1986, 'Experiments on Scalar Dispersion within a Model Plant Canopy. Part I: The Turbulence Structure', *Boundary-Layer Meteorol.* **35**, 21–52.

Raupach, M. R.: 1989, 'Stand Overstorey Processes', *Phil. Trans. R. Soc. Lond.*, **B324**, 175–190.

Raupach, M. R., Finnigan, J. J., and Brunet, Y.: 1989, 'Coherent Eddies in Vegetation Canopies', *Proc. Fourth Australasian Conf. on Heat and Mass Transfer*, Christchurch, New Zealand, 75–90.

Reynolds, W. C. and Hussain, A. K. M. F.: 1972 'The Mechanics of an Organized Wave in Turbulent Shear Flow. Part 3. Theoretical Models and Comparisons with Experiments', *J. Fluid Mech.* **54**, 263–288.

Rotach, M. W.: 1991, 'Turbulence within and above Urban Canopy', ETH Technical Report 45, Geogra. Inst. E. T.H., Zurich, 245 pp.

Rotach, M. W.: 1993a, 'Turbulence Close to a Rough Urban Surface. Part I: Reynolds Stress', *Boundary-Layer Meteorol.* **65**, 1–28.

Rotach, M. W.: 1993b, 'Turbulence Close to a Rough Urban Surface. Part II: Variances and Gradients', *Boundary-Layer Meteorol.* **66**, 75–92.

Roth, M.: 1993, 'Turbulent Transfer Relationships over an Urban Surface. II: Integral Statistics', *Quart. J. Royal Meteorol. Soc.* **119**, 1105–1120.

Roth, M. and Oke, T. R.: 1993, 'Turbulent Transfer Relationships over an Urban Surface. I: Spectral Characteristics', *Quart. J. Royal Meteorol. Soc.* **119**, 1071-1104.

Shiotani, M. and Yamamoto, G.: 1950, 'Atmospheric Turbulence over the Large City', *Geophys. Mag.* **2**, 134–147.

Steyn, D. G.: 1982, 'Turbulence in an Unstable Surface Layer over Suburban Terrain', *Boundary-Layer Meteorol.* **22**, 183–191.

Tutu, N. K. and Chevray, R.: 1975, 'Cross-wire Anemometry in High Intensity Turbulence', *J. Fluid Mech.* **71**, 785–800.

Uno, I., Wakamatsu, S., Ueda, H., and Nakamura, A.: 1988, 'An Observational Study of the Structure of the Nocturnal Urban Boundary Layer', *Boundary-Layer Meteorol.* **45**, 59–82.

Wallace, J. M., Eckelmann, H., and Brodkey, R. S.: 1972, 'The Wall Region in Turbulent Shear Flow', *J. Fluid Mech.* **54**, 39–48.

Wyngaard, J. C., Coté, O. R., and Izumi, Y.: 1971, 'Local Free Convection, Similarity and the Budgets of Shear Stress and Heat Flux', *J. Atmos. Sciences* **28**, 1171–1182.